

Magnetic transitions in triangular antiferromagnets with distorted exchange structure

M. E. Zhitomirsky

*Institute for Solid State Physics, University of Tokyo, Tokyo 106, Japan
and L. D. Landau Institute for Theoretical Physics, Moscow 117334, Russia*

O. A. Petrenko

Department of Physics and Astronomy, McMaster University, Hamilton, Ontario, Canada L8S 4M1

L. A. Prozorova

*P. L. Kapitza Institute for Physical Problems, Moscow 117334, Russia
(Received 21 December 1994; revised manuscript received 20 March 1995)*

Finite-field properties of easy-plane antiferromagnets with deformed stacked triangular lattices are considered. Different distortions of the ideal 120° spin structure at $H = 0$ lead to different types of behavior in a magnetic field applied in the basal plane. For several of them, additional orientational phase transitions are predicted. The theory explains unusual properties of RbMnBr_3 including the low-field phase transition between incommensurate and commensurate spin structures. We report also the results of antiferromagnetic resonance measurements in KNiCl_3 which detect unambiguously two nonequivalent interchain exchange constants in this compound.

I. INTRODUCTION

The effect of frustration is an important topic in current studies of magnetism with particular attention given to the two-dimensional spin systems on a triangular lattice from both theory¹ and experiment.² The family of hexagonal magnetic compounds of ABX_3 type (including CsNiCl_3 , RbNiCl_3 , CsVCl_3 , CsMnBr_3) is an example of *three-dimensional* frustrated systems. In these materials magnetic ions B^{2+} form linear chains along the c axis which are arranged in a regular triangular lattice. Due to frustration of the antiferromagnetic exchange interactions a so-called 120° or triangular spin structure is developed below a magnetic ordering temperature T_N which is typically less than 30 K. This noncollinear structure leads to a variety of new properties not found in ordinary two-sublattice antiferromagnets. Among them there are a new type of critical behavior,^{3,4} splitting of T_N in systems with an easy-axis type of anisotropy,⁵ reorientation by a magnetic field through a collinear phase in compounds with easy-plane anisotropy,⁶ and several new modes of antiferromagnetic resonance with complicated frequency dependences from a magnetic field.⁷⁻¹²

The simple ABX_3 lattice has the space group $P6_3/mmc$, but phase transitions to lower symmetries are fairly common.¹³ It was found that structures of RbFeBr_3 ,^{14,15} below 108 K, of KNiCl_3 ,¹⁶ and of RbMnBr_3 ,¹⁷ at room temperature, are described by the space group $P6_3cm$. In the distorted lattice one of the three adjacent chains is shifted along the c axis relative to the other two chains. The structure of RbMgBr_3 after a phase transition at 449 K is characterized by the space group $P\bar{3}c1$,¹⁸ which corresponds to the shifts of two chains along the c axis by the same distance in opposite directions. RbVBr_3 undergoes a transformation^{19,20}

to an unidentified structure (either $P6_3cm$ or $P\bar{3}c1$) at 90 K.

Generally lattice deformations due to a structural phase transition lead to some modifications of magnetic interactions and, consequently, to a partial lifting of frustration on a stacked triangular lattice. Study of such partially unfrustrated systems is of fundamental interest, because they do not simply correspond to an intermediate case between unfrustrated and frustrated magnets but show novel physical phenomena absent in the two limiting cases. Namely, there were found successive phase transitions in the easy-plane triangular antiferromagnets RbFeBr_3 (Ref. 21) and RbVBr_3 (Refs. 19, 20) at $H = 0$, incommensurate spin structure, two field-induced phase transitions, and a complicated phase diagram with a new type of tetracritical point in RbMnBr_3 .²²⁻²⁶

Previous theoretical considerations of these distorted triangular antiferromagnets have been focused primarily on zero-field properties. The double phase transition in RbFeBr_3 and RbVBr_3 and the incommensurate spin structure in RbMnBr_3 were explained by models with several exchange constants in the basal plane.^{21,27-29} However, their finite-field properties and, in particular, the low-field phase transition in RbMnBr_3 are not properly understood yet.

In the present work we consider phase transitions of distorted triangular ABX_3 -type antiferromagnets in an applied magnetic field at $T = 0$. We show that new orientational phase transitions are possible in these commensurate helimagnets. They include a spin reorientation inside a helix plane rather than a change in the position of this plane as would be for usual spin-flop transitions. Such transitions arise naturally from competing anisotropies in the spin plane provided by small distortions of the exchange structure due to a partial lifting of frustration on the deformed lattice.

The rest of this paper is organized as follows. In Sec. II we briefly describe the Lagrangian approach to the low-energy, long-wavelength dynamics of triangular antiferromagnets developed previously by different authors.^{30–34} This macroscopic theory is used in subsequent sections to study properties of antiferromagnets with distorted exchange structure. Magnetic transitions of triangular antiferromagnets with lattice deformations of “RbFeBr₃-type” are discussed in Sec. III and a distortion of exchange constants in KNiCl₃ is determined from antiferromagnetic resonance measurements. In Sec. IV we adopt a simplified crystal structure for RbMnBr₃ as a stacked triangular lattice subject to uniaxial deformation in the basal plane and show that this gives rise to the observed phase transition in a magnetic field between incommensurate and commensurate spin structures. We also discuss the unique behavior of an antiferromagnetic resonance mode near this transition, which makes this assignment unambiguous.

II. LOW-ENERGY DYNAMICS OF TRIANGULAR ANTIFERROMAGNETS

The magnetic subsystem in undistorted ABX_3 compounds is described by the Hamiltonian

$$\hat{\mathcal{H}} = J \sum_{i,j}^{\text{chains}} \mathbf{S}_i \cdot \mathbf{S}_j + J' \sum_{k,l}^{\text{planes}} \mathbf{S}_k \cdot \mathbf{S}_l + D \sum_i (S_i^z)^2 - \mathbf{H} \sum_i \mathbf{S}_i \quad (1)$$

for spins of magnetic ions B^{2+} placed on a stacked triangular lattice (we put $\gamma = g\mu_B$ to 1 here). The constant of exchange coupling between nearest neighbors along chains J is several orders of magnitude larger than the exchange between adjacent spins in the basal plane J' , which leads to a quasi one-dimensional behavior of the system at high temperatures and significant quantum fluctuations in a three-dimensionally ordered magnetic phase. Single-ion anisotropy is either of the easy-axis type ($D < 0$), as in CsNiCl₃, RbNiCl₃, CsMnI₃, or of the easy-plane type ($D > 0$), as in CsVCl₃, CsMnBr₃, KNiCl₃.

In the absence of anisotropy and a magnetic field, the exchange interactions stabilize at low temperatures a noncollinear triangular spin structure. The adjacent moments along chains are antiparallel, while spins on the neighboring chains in the same plane are at angles of 120° to each other so that the antiferromagnet is subdivided into six sublattices. The order parameter of this magnetic structure is a pair of mutually perpendicular, unit vectors \mathbf{l}_1 and \mathbf{l}_2 , which transform according to the irreducible representation of the space group of the hexagonal Bravais lattice with wave vector \mathbf{Q} :

$$\mathbf{S} \sim \mathbf{l}_1 \cos \mathbf{Q}\mathbf{r} + \mathbf{l}_2 \sin \mathbf{Q}\mathbf{r}, \quad \mathbf{Q} = \left(\frac{4\pi}{3a}, 0, \frac{\pi}{c} \right). \quad (2)$$

The orientation of the spin plane is determined by single-ion anisotropy and an external magnetic field. Their

competition gives rise to a spin-flop transition for either sign of the anisotropy constant D .

The comparison of low-frequency dynamics of triangular antiferromagnets observed in the experiments on antiferromagnetic resonance with predictions of the quasiclassical linear spin-wave theory gives surprisingly good agreement.^{8–11} An explanation of this fact for quantum systems can be given in terms of a phenomenological macroscopic or “hydrodynamic” theory for the low-energy, long-wavelength dynamics.^{30,31} According to this theory the number of low-lying modes of the spin-wave spectrum and their behavior in an applied field depend only on the symmetry of a magnetic system. Therefore, linear spin-wave theory can satisfactorily describe them for quantum antiferromagnets ordered at $T = 0$, though the constants of the magnetic Hamiltonian used in corresponding formulas have to be renormalized to take quantum fluctuations into account.⁶

Since we are interested in phase transitions of triangular antiferromagnets in a magnetic field, we adopt the Lagrangian approach,³¹ which is the most adequate for our purpose and allows to obtain all results analytically. The macroscopic theory^{30,31} predicts for noncollinear antiferromagnets three quasicoustic spin-wave branches whose gaps at $\mathbf{k} = 0$ are determined by a relativistic anisotropy and an external field. The corresponding spins motion is described by time- and position-dependent rotations of the pair $(\mathbf{l}_1, \mathbf{l}_2)$ determined by three angle functions. The resonance spectrum at $T = 0$ (gaps of the acoustic spin waves) can be calculated using the phenomenological Lagrangian $\mathcal{L} = \int \Lambda dV$:

$$\Lambda = \frac{\chi_{\perp}}{2\gamma^2} (\boldsymbol{\Omega} + \gamma \mathbf{H})^2 + \frac{\eta \chi_{\perp}}{2\gamma^2} [\mathbf{n} \cdot (\boldsymbol{\Omega} + \gamma \mathbf{H})]^2 - E_{\text{an}}, \quad (3)$$

where $\mathbf{n} = \mathbf{l}_1 \times \mathbf{l}_2$, χ_{\perp} is the magnetic susceptibility in the spin plane, χ_{\parallel} is the susceptibility in the direction of \mathbf{n} , $\eta = (\chi_{\parallel} - \chi_{\perp})/\chi_{\perp}$, $\boldsymbol{\Omega}$ is the angular velocity of the rotations in spin space, and E_{an} is the anisotropy energy of relativistic and nonlinear susceptibility origins given in the lowest approximation by $E_{\text{an}} = -an_z^2/2$.^{7,12}

The combination in which the angular velocity $\boldsymbol{\Omega}$ and the magnetic field \mathbf{H} enter Eq. (3) is determined by the condition that the total magnetic moment has to be equal to the angular momentum of spin rotation multiplied by a gyromagnetic ratio γ . The Lagrangian density (3) is obtained after that from symmetry arguments.³¹ Analogous expressions were also derived by an exact low-energy, long-wavelength expansion around the Néel-ordered ground state of the quantum Hamiltonian.^{32–34} Parameters of the spin-wave Lagrangian (3) can be obtained either from such microscopic transformation or from their macroscopical interpretation calculating corresponding physical quantities. In the classical limit with $J \gg J'$, $J \gg D$ one finds, at $T = 0$, $\chi_{\perp} = 1/16J$, $\eta = 1$, $a = DS^2$. The Lagrangian (3) adequately describes low-frequency and static properties of triangular antiferromagnets with small anisotropy constant $|D|$ (CsNiCl₃, RbNiCl₃, CsVCl₃).^{7,12} It predicts a spin-flop transition for the case of easy-axis (easy-plane) anisotropy at $H_{\text{s-f}} = |a|/\eta\chi_{\perp} = 16|D|JS^2$, when magnetic field is directed parallel (perpendicular) to the c axis.

However, there is a number of planar antiferromagnets, e.g., CsMnBr₃, RbMnBr₃, KNiCl₃, for which $D > 3J'$. In this case spins do not leave the basal plane for all values of the magnetic field in the basal plane, representing XY -type of behavior.⁶ To understand the corresponding magnetization process, note that for $J' \ll J$ the low-energy degrees of freedom may be represented in terms of the antiferromagnetic vectors \mathbf{L}_i for each of three chains in the magnetic unit cell.³² The total energy of the interaction of a noncollinear structure with a magnetic field is a sum of individual interaction energies of three chains in this approximation. As for ordinary antiferromagnets, each vector \mathbf{L}_i tends to be perpendicular to the field. This is apparently not possible at small magnetic fields where single-ion anisotropy and interchain coupling are dominant. Only one antiferromagnetic vector is directed perpendicular to \mathbf{H} at this field region as shown in Fig. 1. The angle between the another two vectors monotonously decreases and, for $D > 3J'$, the sublattice-flip transition at the critical field

$$H_c = \sqrt{48J'JS^2} \quad (4)$$

takes place before the spin-flop transition at H_{s-f} (see Fig. 1). The subsequent reorientation of spins occurs in a way similar to that for a simple two-sublattice antiferromagnet with easy-plane anisotropy.

The destruction described of the triangular structure with the transition at H_c lies beyond the framework of the macroscopic theory, which considers only small deviations from the exchange configuration (2). Nevertheless, this approach can still be used to consider magnetic properties at small fields $H < H_c$. At zero field there is only one Goldstone mode associated with homogeneous rotations of all spins by an angle φ in the easy plane. The frequencies of the two other relativistic modes ($\omega \sim \sqrt{DJ}$) exceed the characteristic exchange frequency $\sqrt{J'J}$ and cannot be calculated in the low-energy limit. The simplified Lagrangian density, which is a restriction of (3) on a one-dimensional spin space, is given by

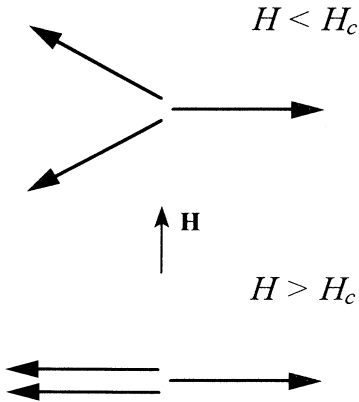


FIG. 1. Spin structures before and after the sublattice-flip transition. Arrows represent antiferromagnetic vectors of three adjacent chains.

$$\Lambda = \frac{\chi_{\parallel}}{2\gamma^2} \dot{\varphi}^2 - E_{\text{an}}, \quad E_{\text{an}} = \frac{\chi_{\perp}}{24} \frac{H^6}{H_c^4} \cos 6\varphi, \quad (5)$$

where the anisotropy is created by a magnetic field applied in the basal plane. Its angular dependence is determined by the first invariant in the expansion of the magnetic energy over powers of H/H_c , which depends on the relative orientation of the field \mathbf{H} and spin vectors: $g[(\mathbf{A}, \mathbf{H})^6 + (\mathbf{A}^*, \mathbf{H})^6]$; here $\mathbf{A} = \mathbf{l}_1 + i\mathbf{l}_2$. The phenomenological parameter g can be easily calculated in the mean-field approximation comparing energies of two symmetrical orientations ($\varphi = 0$ and $\varphi = \pi/2$) of the spin structure with respect to the magnetic field. More strict derivation of the sixfold anisotropy in ABX_3 -type antiferromagnets can be found in Refs. 12 and 34. This consideration of spins motion in terms of a single angle function is analogous to that used previously in the theory of ferromagnetic and antiferromagnetic chains with strong planar anisotropy.³⁵

The minimum of $E_{\text{an}}(\varphi)$ is achieved for $\varphi = \pi/2$, which corresponds to the low-field spin configuration in Fig. 1. Small homogeneous oscillations near this equilibrium position are described by the equation of motion $d(\partial\Lambda/\partial\dot{\varphi})/dt = \partial\Lambda/\partial\varphi$, which gives their frequency

$$\omega = \gamma \frac{H^3}{H_c^2} \sqrt{\frac{3}{2(1+\eta)}}. \quad (6)$$

Such a dependence of the resonance frequency with magnetic field was observed in CsMnBr₃.¹⁰ Though at fields $H \sim H_c$ sublattices deviate significantly from the 120° structure, the expression (6) is close to the exact numerical results by Chubukov⁶ for $H < 0.7H_c$. Moreover, the accuracy of (6) grows with the increasing XY character of spins, that is, with increasing ratio $D/3J'$. Therefore, considering transitions in the noncollinear phase of distorted triangular antiferromagnets at $H < H_c$ we will base our analysis on some modifications of the simple spin-wave Lagrangian (5). For the collinear phase at $H > H_c$ Eq. (6) is replaced by a usual paramagnetic dependence $\omega = \gamma H$ known for two-sublattice antiferromagnets.

III. MAGNETIC PROPERTIES OF RbFeBr₃-TYPE MODIFIED ANTIFERROMAGNETS

Near the melting point all hexagonal ABX_3 crystals have an undistorted structure described by the $P6_3/mmc$ space group. Phase transitions to lattices of lower symmetry with decreasing temperature are characterized usually by displacements of chains of magnetic atoms as a whole without deformation so that the intrachain distance between spins remains unchanged. The typical structural transition to the lattice of $P6_3cm$ space group is accompanied by the shift of one from the three adjacent chains upward along the c axis while the two others shift downward, keeping the crystal center of mass undistorted. Distortions of this type were found in the low-temperature phase of RbFeBr₃,^{14,15} at room temperature in KNiCl₃ (Ref. 16) and in RbMnBr₃ (Ref. 17) and,

probably, in RbVBr_3 .²⁰ The crystal unit cell in the basal plane is enlarged to become $\sqrt{3}a \times \sqrt{3}a$ (Fig. 2), preserving the hexagonal symmetry. Because chains are shifted usually on a small distance from the basal plane [$\sim 0.5 \text{ \AA}$ in RbFeBr_3 (Ref. 14)], magnetic properties may be considered by placing spins on the same stacked triangular lattice and changing interactions in the Hamiltonian (1) in accordance with a reduced symmetry of the crystal structure.

On the RbFeBr_3 -type modified lattice there are two kinds of exchange coupling constants between nearest neighbors in the basal plane: J' for pairs on equivalent A_1 - A_2 sites and J'_1 for pairs on A - B sites, as shown in Fig. 2. The Hamiltonian of this centered honeycomb model (in terms of Zhang *et al.*²⁹) is obtained by the evident replacement of the second term on the right-hand side (RHS) of Eq. (1):

$$J' \sum_{i,j}^{A-A} \mathbf{S}_i \cdot \mathbf{S}_j + J'_1 \sum_{k,l}^{A-B} \mathbf{S}_k \cdot \mathbf{S}_l. \quad (7)$$

The other type of structural transition in the hexagonal lattice is realized in the nonmagnetic compound RbMgBr_3 (Ref. 18) and consists in the upward shift of the first chain along the c axis and the opposite shift of the second chain. Considering again changes only in exchange interactions we can describe a spin model with the lattice of this type by the same Hamiltonian of the centered honeycomb model with two coupling constants in the basal plane. In this case atoms on B sites lie in the plane of Fig. 2, while atoms on A_1 and A_2 sites are displaced forward and back, respectively.

At zero field the classical ground state obtained by minimization of (7) is a planar spin structure presented in Fig. 3 with antiparallel spins along the c direction. The angle θ is given for $J'_1 < 2J'$ by

$$\cos \theta = \frac{J'_1}{2J'}, \quad (8)$$

whereas for $J'_1 > 2J'$ the structure is collinear ($\theta = 0$).²⁹ The characteristic parameter of the problem is the relative difference between exchange constants $\delta = (J'_1/J' - 1)$. Depending on the sign of δ there are possible two types of the distorted triangular structure: I, with

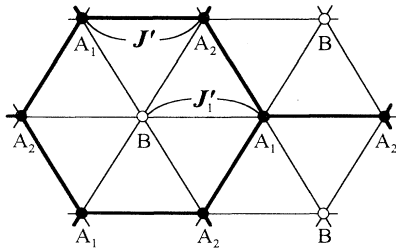


FIG. 2. The schematic crystal structure and exchange constants in the basal plane for hexagonal antiferromagnets of $P6_3cm$ and $P\bar{3}c1$ space groups. The dark bonds are J' ; the light bonds are J'_1 .

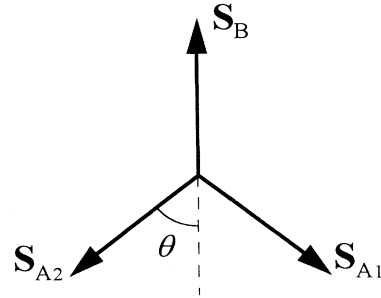


FIG. 3. The relative orientation of spins on adjacent chains at $H = 0$ for an antiferromagnet on the deformed lattice of RbFeBr_3 type.

$\theta < 120^\circ$ ($0 < \delta < 1$), and II, with $\theta > 120^\circ$ ($\delta < 0$). We will show that reorientation processes in magnetic field are different for them.

Since the superexchange interaction J' originates from the overlap of electron orbits of B^{2+} atoms with valence p orbits of intermediate X atoms, it depends in a complicated way from the interatomic distances and bond angles. It is difficult to predict in advance the relation between J' and J'_1 for deformed lattices of the $P6_3cm$ space group, where A - B distance is larger than A_1 - A_2 , as well as for lattices of the $P\bar{3}c1$ symmetry, where spacing relations are opposite. Therefore, for each lattice we must consider both types of the distorted spin structure.

Without field the spin ordering occurs in two steps in each case with an additional intermediate collinear phase between T_{N1} and T_{N2} ($\Delta T_N/T_N \sim |\delta|$) which is either ferrimagnetic ($\delta > 0$) or partially disordered ($\delta < 0$).²⁸

At low temperatures magnetic field applied in the basal plane leads, as in the case of ordinary triangular antiferromagnets (Sec. II), to a transition into the collinear phase at the critical field H_c , which depends on both J' and J'_1 .⁹ However, if the relative difference between J' and J'_1 is small, one may still use the old expression (4) neglecting corrections of the order of $|\delta|$ to H_c . We consider in this approximation magnetic properties of the noncollinear phase at fields $H \lesssim H_c$.

The asymmetry of the magnetic structure with a preferable direction in the spin plane results in the anisotropy of inplane susceptibility. For $|\delta| \ll 1$ this anisotropy is represented by the invariant $[(\mathbf{H}, \mathbf{A})^2 + (\mathbf{H}, \mathbf{A}^*)^2]$, which arises due to the partial breaking of translation symmetry of the original Bravais lattice. Comparing mean-field energies for two perpendicular orientations of the spin system we can express the anisotropic part of magnetic energy associated with the distortions as

$$E'_{\text{an}} = \frac{\chi_{\perp}}{3} \delta ((\mathbf{H}\mathbf{1}_1)^2 - (\mathbf{H}\mathbf{1}_2)^2). \quad (9)$$

The different sign of E'_{an} for the above two types of distorted triangular structure can be easily understood in terms of interactions of individual chains with magnetic field (Sec. II). The whole anisotropy energy of the spin system in the magnetic field is given by

$$E_{\text{an}} = \frac{\chi_{\perp}}{3} H^2 \left(\delta \cos 2\varphi + \frac{H^4}{8H_c^4} \cos 6\varphi \right). \quad (10)$$

For a type-I distorted triangular structure both anisotropies in (10) favor the same orientation of spins. The only difference from the case of perfect triangular antiferromagnets (Fig. 1) is that, due to the partial lifting of frustration, it is the antiferromagnetic vector of B chains \mathbf{L}_B which is directed perpendicularly to \mathbf{H} . This corresponds to $\varphi = \pi/2$ at the equilibrium and substituting (10) into (5) we find the resonance frequency:

$$\omega = \gamma H \left(\frac{4\delta/3 + 3H^4/2H_c^4}{1 + \eta} \right)^{1/2}, \quad (11)$$

which has a linear asymptote for small H in contrast to (6). The formula (11) is valid for small δ at the field range $0 < H \lesssim 0.7H_c$ and incorporates partially quantum fluctuations through renormalization of η . The behavior of $\omega(H)$ in case I including the region near H_c was found numerically in the classical limit ($\eta = 1$) by Tanaka *et al.*⁹ However, properties of the type-II distorted triangular structure were considered incorrectly there.

In case II ($\delta < 0$), the anisotropy (9) gives a different spin orientation at low fields with the pair of sublattices on B chains directed along \mathbf{H} (Fig. 4). Such a configuration is energetically unfavorable at higher fields, where the sixfold anisotropy becomes significant. Rotation of the spin system between the two limiting orientations $\varphi = 0$ and $\varphi = \pi/2$ occurs with an additional phase transition. Minimizing (10) we find the following sequence of equilibrium states

$$\begin{aligned} \varphi = 0 & \quad \text{for } H < H^* = H_c \left(\frac{8}{9} |\delta| \right)^{1/4}, \\ \varphi = \frac{1}{2} \arcsin \left[\frac{3}{4} \left(1 - \frac{H^{*4}}{H^4} \right) \right]^{1/2} & \quad \text{for } H > H^*. \end{aligned} \quad (12)$$

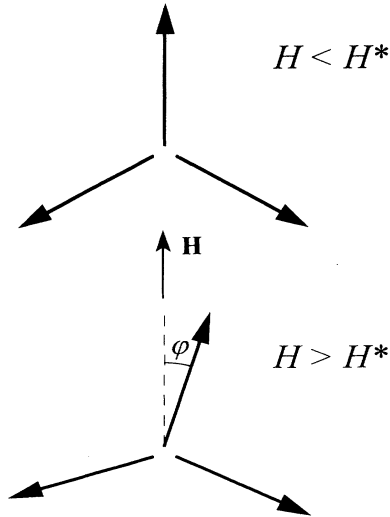


FIG. 4. The behavior of the triangular spin structure with $\theta > 60^\circ$ at small fields.

The phase transition at $H = H^*$ is of second order. Taking for the estimation $\delta = -0.05$ we obtain, from (12), $H^* = 0.46H_c$. Thus already very small changes in the exchange constants alter significantly the behavior of the triangular antiferromagnet in a magnetic field. The existence of the orientational phase transition at $H = H^*$ reveals itself as a small change of slope in the magnetization curve corresponding to the jump $\Delta\chi/\chi = 2|\delta|$ in susceptibility. The most pronounced sign of this phase transition, however, can be seen in the behavior of the lowest branch in the resonance spectrum with magnetic field

$$\begin{aligned} \omega &= \gamma H \left(\frac{3(H^{*4} - H^4)}{2(1 + \eta)H_c^4} \right)^{1/2} \quad \text{for } H < H^*, \\ \omega &= \gamma H \left(\frac{3(H^4 - H^{*4})}{(1 + \eta)H_c^4} \sqrt{\frac{1}{4} + \frac{3H^{*4}}{4H^4}} \right)^{1/2} \quad \text{for } H > H^*, \end{aligned} \quad (13)$$

which corresponds to the disappearance of the gap in the spin-wave spectrum at $H = H^*$ (see Fig. 5).

We have derived expressions (12) and (13) in the limit $|\delta| \ll 1$. They are not appropriate when H^* becomes equal or exceeds the actual value of critical field for the sublattice-flip transition determined by $\tilde{H}_c^2 = H_c^2(\sqrt{1 + 3(1 - |\delta|)^2} - 1)$,⁹ that is, for $|\delta| > 0.3$. To find H^* in this case a numerical investigation of the original Hamiltonian is required.

There are three hexagonal antiferromagnets RbFeBr₃, RbVBr₃, and KNiCl₃ for which these results can be applied. The antiferromagnetic resonance has been measured only in KNiCl₃. In Fig. 6 we present experimental data obtained by Tanaka *et al.*⁹ along with the results of our measurements. Obviously, the behavior of the lowest branch of the antiferromagnetic resonance $\omega(H)$ corresponds to case I ($J'_1 > J'$). The fit of the experimental points at fields $H < 0.7H_c$ with $\eta \approx 0.6$ and $H_c = 23$ kOe (Ref. 36) and $\gamma = 3.14$ GHz/kOe (Ref. 9)

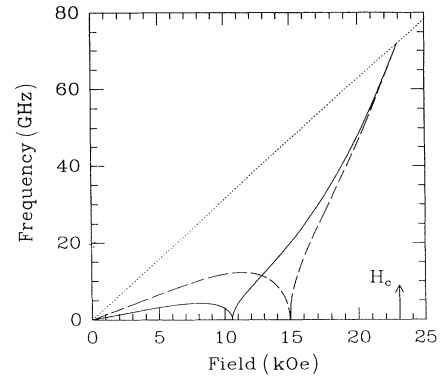


FIG. 5. The behavior of the lowest branch of resonance spectrum for the type-II distorted triangular structure with $\delta = -0.05$ (solid line) and with $\delta = -0.2$ (dashed line). Dotted line corresponds to $\omega = \gamma H$ in the collinear phase. Parameters H_c , γ and η are chosen the same as in KNiCl₃ (see text).

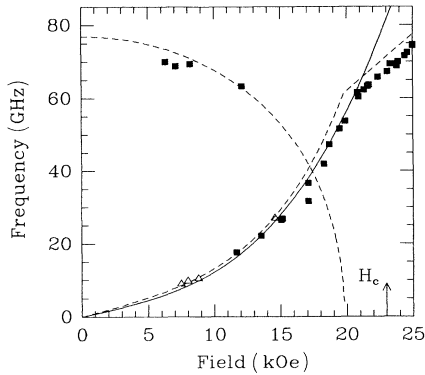


FIG. 6. Spectrum of antiferromagnetic resonance in KNiCl_3 at $T = 1.3$ K. Solid squares represent the results of our measurements. Four points at low field and high frequency correspond to the exchange branch of resonance which is not described by the macroscopic theory. Open symbols and dashed lines are experimental results and theory respectively from Ref. 9. The solid line is drawn using Eq. (10) with parameters from the text (Ref. 37). It fits the experimental points for fields $H < 0.7H_c = 16.1$ kOe.

gives $\delta = 0.08 \pm 0.01$.³⁷ Quantum effects are important in KNiCl_3 because the relative difference between transverse and inplane susceptibilities η deviates significantly from its classical value $\eta = 1$. As a result, the estimated value for δ is smaller than that of Tanaka *et al.*,⁹ who neglected these effects. Also, due to the extremely large anisotropy $D \approx 200J'$ in this material³⁶ results obtained in the XY approximation are in good agreement with experimental data on KNiCl_3 practically for all fields $0 < H < H_c$.

On the other hand the magnetization measurements³⁶ did not show any evidence for the splitting of the Néel temperature $T_N = 8.6$ K with an accuracy of 0.15 K. It should be noted in this connection that the investigation of dielectric properties of KNiCl_3 revealed up to four successive ferroelectric transitions.³⁸ Generally, they can be not only of the displacive but also of the order-disorder type. The latter is confirmed by an electron diffraction study³⁹ interpreted as the existence of a certain degree of structural disorder in the vertical shifts of the magnetic chains. Therefore, the RbFeBr_3 -type deformations in the crystal lattice of KNiCl_3 can be changed even within the temperature interval of the antiferromagnetic ordering.

In RbFeBr_3 and RbVBr_3 , instead, a large splitting of the Néel temperature was observed with $T_{N1} = 5.6$ K, $T_{N2} = 2$ K (Ref. 21) and $T_{N1} = 28$ K, $T_{N2} = 21$ K (Ref. 20), respectively. The convincing arguments in favor of one of the two types of the deformed triangular structure were suggested only for RbVBr_3 by Tanaka and Kakurai²⁰ on the basis of neutron scattering measurements in the intermediate phase. From the temperature behavior of the intensity of Bragg peaks they concluded that the spin ordering between T_{N1} and T_{N2} has a partially disordered collinear structure. They estimated also the angle between sublattices in the distorted spin triangle at $T = 0$ as $\theta = 73^\circ$ and, thus, $J'_1/J' = 0.6$ or

$\delta = -0.4$. Such a deformation of the 120° structure is too large to be described by our approximate formulas. However, the phase transition field H^* still has to exist because of the different symmetries of the low-field ($H \rightarrow H^*$) and high-field ($H \lesssim H_c$) phases and can be determined from the measurements of resonance or magnetization in RbVBr_3 at low temperatures. Adachi *et al.*²¹ also supposed the second type of deformation of the spin structure in RbFeBr_3 at $T = 0$ and found $J'_1/J' = 0.85$ from the observed splitting of the Néel temperature. The field of the orientational phase transition can be estimated as $H^* \approx 0.6H_c$ in this case.

IV. DISTORTED TRIANGULAR STRUCTURE IN RbMnBr_3

The macroscopic properties of RbMnBr_3 , another easy-plane magnetic compound with a deformed stacked triangular lattice, differ significantly from those we have discussed in the previous section. The experimental results²² on the spectrum of antiferromagnetic resonance in RbMnBr_3 at $T = 1.3$ K ($T_N = 8.8$ K) are reproduced in Fig. 7. A low-frequency resonance branch analogous to those in CsMnBr_3 and KNiCl_3 exists in magnetic fields $H > 30$ kOe until the transition with a spin flip of the two pairs of sublattices takes place at $H_c = 39$ kOe. However, for $H < 25$ kOe there is no observable low-frequency resonance absorption. The disappearance of a resonance signal in the field region $25 < H < 30$ kOe is accompanied by a hysteresis in its intensity and shape, and, simultaneously, with a small hysteresis in the magnetization curve.^{23,26} This seemingly unique effect is connected with the more complicated magnetic structure found in RbMnBr_3 .

Single-crystal neutron diffraction measurements on RbMnBr_3 (Refs. 24, 25) show an incommensurate magnetic structure at low temperatures and fields. While the commensurate structures discussed in Secs. II and III give rise to a magnetic Bragg peak at $(\frac{1}{3}, \frac{1}{3}, 1)$, indexed

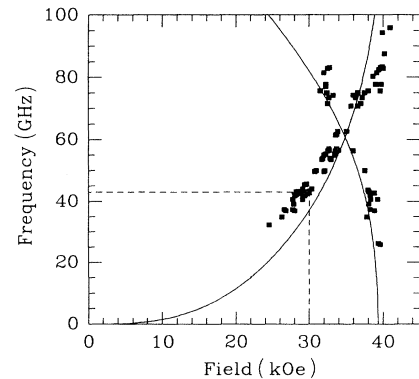


FIG. 7. Spectrum of antiferromagnetic resonance in RbMnBr_3 at $T = 1.3$ K from Ref. 22. The dashed line marks the region where the hysteresis of the intensity and shape of resonance absorption signal was observed.

in the $a \times a$ lattice, the neutrons data²⁵ give two triads of magnetic peaks in the $(hk1)$ plane near to $(\frac{1}{3}, \frac{1}{3}, 1)$. These triads correspond to spiral structures with turn angles of 128° and 142° which are greater than the helix angle of 120° needed for the commensurate structure.

The crystal structure of RbMnBr_3 near the Néel temperature is known with less certainty. The birefringence study of Kato *et al.*⁴⁰ is compatible with orthorhombic distortions below 220 K in addition to the room temperature RbFeBr_3 -type modifications of the crystal lattice.¹⁷ Recently, the existence of orthorhombic distortions at $T = 12$ K has been demonstrated in powder neutron scattering experiments.⁴¹ Whether or not they coincide with RbFeBr_3 -type crystal deformations in the antiferromagnetic phase is still in question.

The appearance of an incommensurate helical spin order at zero field was attributed to orthorhombic deformations of the underlying hexagonal lattice in a number of papers.^{27,29} Though the corresponding spin model might be too simplified to explain the real complicated magnetic structure of RbMnBr_3 , we show that the destruction of such an incommensurate spin spiral by a magnetic field provides an explanation of the low-field phase transition observed in this compound.

We consider spins on a stacked triangular lattice subjected to a small uniaxial deformation along one of the hexagonal directions in the basal plane. Due to the relative change of interatomic distances, one can expect a deformation of inplane exchange interactions as shown in Fig. 8. Horizontal spin bonds are J' , while bonds between rows are J'_1 . The Hamiltonian of this row model of Zhang *et al.*²⁹ is obtained by the replacement of the second sum on the RHS of Eq. (1) on

$$J' \sum_{i,j}^{\text{intrarow}} \mathbf{S}_i \cdot \mathbf{S}_j + J'_1 \sum_{k,l}^{\text{interrow}} \mathbf{S}_k \cdot \mathbf{S}_l. \quad (14)$$

Note that the hexagonal symmetry of the lattice is broken in this model and the wave vector of the commensurate structure (2) does not correspond to a special symmetrical point in the Brillouin zone.

To find the ground state of the system at zero field one has to substitute a helical spin configuration of general form $\mathbf{S}(\mathbf{r}) = (S \cos(\mathbf{k}\mathbf{r}), S \sin(\mathbf{k}\mathbf{r}), 0)$ in the Hamiltonian of the row model. The energy per spin is given by the Fourier transform of the exchange energy:

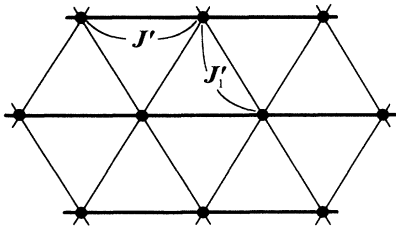


FIG. 8. The schematic crystal structure and exchange constants in the row model for RbMnBr_3 .

$$\varepsilon(\mathbf{k}) = 2JS^2 \cos k_z c + 2J'S^2 \left(\cos k_x a + 2 \frac{J'_1}{J'} \cos \frac{k_x a}{2} \cos \frac{\sqrt{3}}{2} k_y a \right). \quad (15)$$

Minimizing $\varepsilon(\mathbf{k})$ one obtains $k_y = 0$, $k_z = \pi/c$, while k_x is given by

$$\cos \frac{k_x a}{2} = - \frac{J'_1}{2J'}. \quad (16)$$

If the relative deviation of exchange constants from the old value $\delta = (J'_1/J' - 1)$ is small, the wave vector of the incommensurate spin structure can be represented as

$$\mathbf{k} = \mathbf{Q} + \mathbf{q}, \quad \mathbf{q} = \left(\frac{2}{\sqrt{3}} \frac{\delta}{a}, 0, 0 \right). \quad (17)$$

This expression allows us to consider the spin configuration in the continuum approximation as a slow modulation of the perfect triangular structure (2). It is described locally by the vector pair $(\mathbf{l}_1, \mathbf{l}_2)$, which rotates from point to point by the angle $\varphi = \mathbf{q} \cdot \mathbf{r}$. The direction of the modulation vector \mathbf{q} is uniquely determined by the direction of external deformation of the triangular lattice. Three types of structural domains with equivalent directions of orthorhombic distortions yield a triad of peaks with threefold symmetry for incommensurate wave vectors surrounding commensurate position at \mathbf{Q} .

In the continuum approximation the energy (15) of the incommensurate magnetic structure is given by a sum of two terms, one of which represents rigidity of the triangular structure^{32,33}

$$JS^2 c^2 \left(\frac{d\varphi}{dz} \right)^2 + \frac{3}{4} J' S^2 a^2 \left[\left(\frac{d\varphi}{dx} \right)^2 + \left(\frac{d\varphi}{dy} \right)^2 \right], \quad (18)$$

while the second is the Lifshitz invariant,

$$- \sqrt{3} J' S^2 a \delta \frac{d\varphi}{dx}. \quad (19)$$

An in-plane magnetic field produces a hexagonal anisotropy energy (5) with the critical field of the flip of two sublattices H_c given in the row model by

$$H_c = \sqrt{16(J' + 2J'_1)JS^2}. \quad (20)$$

Then, if we omit gradients along \hat{y} and \hat{z} , the energy density per spin is written as

$$E = \frac{3}{4} J' S^2 a^2 \left(\frac{d\varphi}{dx} \right)^2 - \sqrt{3} J' S^2 a \delta \frac{d\varphi}{dx} + \frac{\chi_\perp}{24} \frac{H^6}{H_c^4} \cos 6\varphi. \quad (21)$$

The functional (21) has a form typical for many other systems with a weak incommensurability.⁴² A transition in such systems occurs because of the competition between the Lifshitz term and the anisotropy which favors the commensurate phase. The angle function $\varphi_0(x)$ of the ground state satisfies the sine-Gordon equation

$$a^2 \varphi_0''(x) + \frac{H^6}{2H_c^6} \sin 6\varphi_0 = 0. \quad (22)$$

With increasing magnetic field its solution gradually evolves from the perfect sinusoidal structure $\varphi_0(x) = qx$ as

$$\varphi_0(x) = \frac{1}{3} am[(x + x_0)/l] \quad (23)$$

until the critical field is reached (am denotes elliptic amplitude; l is proportional to its modulus).⁴² This field

$$H^* = H_c \sqrt[3]{\pi|\delta|} \quad (24)$$

corresponds to a lock-in phase transition into the commensurate state $\varphi = \pi/2$. The deviations of the spin spiral (23) from the sinusoidal structure are very small at almost all fields $H < H^*$ and the helix period is $\lambda = (2\pi/q)(1 + 5\pi^4 H^{12}/512H^{*12})$. In the vicinity of H^* these deviations become large and the incommensurate structure transforms into an equidistant set of domain walls between regions, where spins are ordered with the commensurate wave vector \mathbf{Q} . The period of the spiral is given by $\lambda = (4/\pi q) \ln[H^*/3(H^* - H)]$ in this region, while the actual interwall spacing is 3 times smaller than λ , due to the existence of three types of domains.

The spectrum of small oscillations can be found by including in (21) the kinetic energy from (5) and linearizing the equation of motion for a small amplitude ψ , $\varphi(x, t) = \varphi_0(x) + \psi(x, t)$ (see, e.g., Ref. 43). In order to describe the antiferromagnetic resonance, we need only to determine the form of the solution at small wave vectors. It follows from Eqs. (21)–(23) that the ground state $\varphi_0(x)$ is degenerate with respect to an arbitrary translation along the \hat{x} axis (to a change of x_0). Therefore, the spectrum of small oscillations is always acoustic in character for all $H < H^*$.⁴³ As a result, the frequency of homogeneous antiferromagnetic resonance is *exactly zero* until the transition into the commensurate phase, after which the frequency is given by Eq. (6).

In a real system this ideal behavior is smeared near H^* by a strong pinning of local domain walls on different sample imperfections and the phase transition into the commensurate phase is accompanied by hysteresis effects.^{22–25}

If, in addition, there are deformations of the RbFeBr₃ type, the hexagonal anisotropy in (21) should be replaced by (10). This modification does not change the above conclusions about the phase transition to the commensurate phase and the disappearance of the resonance at $H < H^*$, while the actual expressions for H^* and the spatial dependence $\varphi_0(x)$ become more complicated. These deformations would give rise also to deviations of the resonance frequency from (6) in the commensurate phase ($H > H^*$).

We take from the magnetization measurements²³ $H^* = 27$ kOe, $H_c = 39$ kOe for RbMnBr₃ and substituting them into (24) obtain $\delta \approx -0.1$. The sign of δ is determined by the sign of the deviation of the helix angle from 120° known from neutron scattering experiments,^{24,25} which give also close values for critical fields. The angle

between adjacent spins can be estimated as 127° for this value of δ . However, there are several discrepancies with neutron data,²⁵ which show two triads of peaks around the commensurate position instead of a one triad, as in our model. The commensurate wave vector of the high-field phases ($H > H^*$) is also attributed to be different from \mathbf{Q} . Nevertheless, we believe that the characteristic behavior of the lowest branch of antiferromagnetic resonance (spin-wave gap) at $H > H^*$ together with the subsequent flip of two pairs of sublattices at H_c indicated by the fall of the exchange branch (Fig. 7) suggests the conventional triangular spin structure in this field region described by six sublattices.⁶ Whether these discrepancies can be resolved involving a more complicated crystal structure of RbMnBr₃ as well as an explanation of the whole H - T phase diagram^{25,26} in terms of the present model requires additional investigations.

V. CONCLUSIONS

The phase transitions of the hexagonal easy-plane antiferromagnets with partially released frustration due to deformations of exchange bonds were studied in the framework of the macroscopic theory. Using symmetry arguments we have shown that different types of distortions of the ideal triangular structure in hexagonal easy-plane antiferromagnets (previously studied^{27–29} at $H = 0$) can be distinguished unambiguously by their behavior in a magnetic field applied in the spin plane. For the first two types of distortions described by the Hamiltonian of the centered honeycomb model an additional anisotropy occurs in a magnetic field. Its competition with the sixfold magnetic anisotropy of the original triangular structure can result in a reorientational transition of second order. The absence of such a transition in KNiCl₃, as shown clearly by our resonance measurements, together with the linear dependence of $\omega(H)$ at small H points to the first type of distortion of the exchange triangular structure. Analogous investigations of RbFeBr₃ and RbVBr₃ will provide explicit information about distortions of the spin structure in these compounds too. The third type of nearly triangular spin structure represented by the incommensurate spin spiral of the row model undergoes a lock-in transition to the commensurate noncollinear phase and, then, a second-order transition to the collinear phase, as was observed in RbMnBr₃ with a magnetic field in the basal plane.

The advantage of the macroscopic approach adopted in the present work is the possibility of an analytical description of complicated distorted spin structures, reducing them either to well-studied systems with weak incommensurability (Sec. IV) or to very simple systems with competing anisotropies (Sec. III). However, all predictions of this method are restricted by small (about 20%) deformations of the exchange coupling constants. The obtained results remain valid for systems with small easy-plane anisotropy ($D < 3J'$), if the condition $H^* < H_{s-f}$ is satisfied. In contrast, the magnetic properties of the two-dimensional partially unfrustrated models²⁹ will be

similar to those of the quasi one-dimensional ferromagnet CsCuCl_3 (with antiferromagnetic interchain exchange),⁴⁴ rather than to the properties discussed here for quasi one-dimensional antiferromagnets.

An interesting feature connected with the complicated nature of superexchange interactions in ABX_3 compounds and observed in both KNiCl_3 and RbMnBr_3 is an unusual dependence of exchange constants on the deformed bonds from the interatomic spacing. Namely, in KNiCl_3 the exchange grows ($J'_1 > J'$) with the increase of distances between magnetic ions for RbFeBr_3 -type deformations, while in RbMnBr_3 it becomes smaller ($J'_1 < J'$) with orthorhombic compression⁴¹ of the lattice in one of the hexagonal directions.

ACKNOWLEDGMENTS

We are grateful to M. F. Collins and I. A. Zaliznyak for interesting discussions, to S. S. Sosin for help in measurements, and to M. F. Collins and K. Ueda for many valuable remarks on the manuscript. M.E.Zh. is indebted for the hospitality to M. Okazaki and to the Institute of Materials Science, University of Tsukuba where part of this work was done. He acknowledges financial support from the Japan Society for the Promotion of Science. O.A.P. thanks Natural Sciences and Engineering Research Council of Canada for financial support. The work of L.A.P. was supported in part by Grant No. M3K000 from the International Science Foundation.

- ¹ D. H. Lee, J. D. Joannopoulos, J. W. Negele, and D. P. Landau, *Phys. Rev. Lett.* **52**, 433 (1984); *Phys. Rev. B* **33**, 450 (1986); S. E. Korshunov, *J. Phys. C* **19**, 5927 (1986); E. Rastelli, A. Tassi, A. Pimpinelli, and S. Sedazari, *Phys. Rev. B* **45**, 7936 (1992).
- ² L. P. Regnault and J. Rossat-Mignod, in *Magnetic Properties of Layered Transition Metal Compounds*, edited by L. J. de Jong (Kluwer, Dordrecht, Netherlands, 1990), p. 271.
- ³ T. E. Mason, M. F. Collins, and B. D. Gaulin, *J. Phys. C* **20**, L945 (1987).
- ⁴ H. Kawamura, *Phys. Rev. B* **38**, 4916 (1988).
- ⁵ X. Zhu and M. B. Walker, *Phys. Rev. B* **36**, 3830 (1987); M. L. Plumer, A. Caillé, and K. Hood, *ibid.* **39**, 4489 (1989).
- ⁶ A. V. Chubukov, *J. Phys. C* **21**, L441 (1988).
- ⁷ I. A. Zaliznyak, V. I. Marchenko, S. V. Petrov, L. A. Prozorova, and A. V. Chubukov, *Pis'ma Zh. Eksp. Teor. Fiz.* **47**, 172 (1988) [*JETP Lett.* **47**, 211 (1988)].
- ⁸ H. Tanaka, S. Teraoka, E. Kakakashi, K. Iio, and K. Nagata, *J. Phys. Soc. Jpn.* **57**, 3979 (1988).
- ⁹ H. Tanaka, Y. Kaahawa, T. Hasegawa, M. Igarashi, S. Teraoka, K. Iio, and K. Nagata, *J. Phys. Soc. Jpn.* **58**, 2930 (1989).
- ¹⁰ I. A. Zaliznyak, L. A. Prozorova, and S. V. Petrov, *Zh. Eksp. Teor. Fiz.* **97**, 359 (1990) [*Sov. Phys. JETP* **70**, 203 (1990)]; O. A. Petrenko, S. V. Petrov, and L. A. Prozorova, *ibid.* **98**, 727 (1990) [*ibid.* **71**, 406 (1990)].
- ¹¹ W. Palme, H. Krieglstein, O. Born, A. Chennaoui, and B. Lüthi, *Z. Phys. B* **92**, 1 (1993).
- ¹² S. I. Abarzhi, M. E. Zhitomirsky, O. A. Petrenko, S. V. Petrov, and L. A. Prozorova, *Zh. Eksp. Teor. Fiz.* **104**, 3232 (1993) [*Sov. Phys. JETP* **77**, 521 (1993)].
- ¹³ J. L. Mañes, M. J. Tello, and J. M. Pérez-Mato, *Phys. Rev. B* **26**, 250 (1982).
- ¹⁴ M. Eibschütz, G. R. Davidson, and D. E. Cox, in *Magnetism and Magnetic Materials*, AIP Conf. Proc. No. 18, edited by C. D. Graham and J. J. Rhyne (AIP, New York, 1974), p. 386.
- ¹⁵ A. Harrison and D. Visser, *J. Phys. Condens. Matter* **1**, 733 (1989).
- ¹⁶ D. Visser, G. C. Verschoor, and D. J. W. Ijdo, *Acta Crystallogr. B* **36**, 28 (1980).
- ¹⁷ H. von Fink and H.-J. Seifert, *Acta Crystallogr. B* **38**, 912 (1982).
- ¹⁸ H.-J. Seifert and J. Wasel-Neilen, *Rev. Chim. Minèr.* **14**, 503 (1977).
- ¹⁹ A. Hauser, U. Falk, P. Fischer, and H. U. Güdel, *J. Solid State Chem.* **56**, 343 (1985).
- ²⁰ H. Tanaka and K. Kakurai, *J. Phys. Soc. Jpn.* **63**, 3412 (1994).
- ²¹ K. Adachi, K. Takeda, F. Matsubara, M. Menate, and T. Haseda, *J. Phys. Soc. Jpn.* **52**, 2202 (1983).
- ²² I. M. Vitebskii, O. A. Petrenko, S. V. Petrov, and L. A. Prozorova, *Zh. Eksp. Teor. Fiz.* **103**, 326 (1993) [*Sov. Phys. JETP* **76**, 178 (1993)].
- ²³ A. N. Bazhan, I. A. Zaliznyak, D. V. Nikiforov, O. A. Petrenko, S. V. Petrov, and L. A. Prozorova, *Zh. Eksp. Teor. Fiz.* **103**, 691 (1993) [*Sov. Phys. JETP* **76**, 342 (1993)].
- ²⁴ T. Kato, T. Ishii, Y. Ajiro, T. Asano, and S. Kawano, *J. Phys. Soc. Jpn.* **62**, 3384 (1993).
- ²⁵ L. Heller, M. F. Collins, Y. S. Yang, and B. Collier, *Phys. Rev. B* **49**, 1104 (1994).
- ²⁶ T. Asano, Y. Ajiro, M. Mekata, H. A. Katori, and T. Goto, *Physica B* **201**, 75 (1994).
- ²⁷ H. Kawamura, *Prog. Theor. Phys. Suppl.* **101**, 545 (1990).
- ²⁸ M. L. Plumer, A. Caillé, and H. Kawamura, *Phys. Rev. B* **44**, 4461 (1991).
- ²⁹ W. Zhang, W. M. Saslow, and M. Gabay, *Phys. Rev. B* **44**, 5129 (1991); W. Zhang, W. M. Saslow, M. Gabay, and M. Benakli, *ibid.* **48**, 10204 (1993).
- ³⁰ B. I. Halperin and P. C. Hohenberg, *Phys. Rev.* **188**, 898 (1969); B. I. Halperin and W. M. Saslow, *Phys. Rev. B* **16**, 2154 (1977).
- ³¹ A. F. Andreev and V. I. Marchenko, *Usp. Fiz. Nauk* **130**, 39 (1980) [*Sov. Phys. Usp.* **23**, 21 (1980)].
- ³² I. Affleck, *Phys. Rev. Lett.* **62**, 474 (1989).
- ³³ T. Dombre and N. Read, *Phys. Rev. B* **39**, 6797 (1989).
- ³⁴ T. Ohyama and H. Shiba, *J. Phys. Soc. Jpn.* **61**, 4174 (1992).
- ³⁵ H. J. Mikeska, *J. Phys. C* **11**, L29 (1978); **13**, 2913 (1980).
- ³⁶ O. A. Petrenko, M. F. Collins, C. V. Stager, and Z. Tun, *Phys. Rev. B* **51**, 9015 (1995).
- ³⁷ To achieve better agreement with experimental data it is necessary to take into account also the next-order mixed term $-(\chi_{\perp} H^4 / 3H_c^2) \delta \cos 4\varphi$ in the expansion of E_{an} over powers of δ and H/H_c .
- ³⁸ K. Machida, T. Mitsui, T. Kato, and K. Iio, *Solid State Commun.* **91**, 17 (1994).
- ³⁹ D. Visser and A. Prodan, *Phys. Status Solidi A* **58**, 481

- (1980).
- ⁴⁰ T. Kato, K. Iio, T. Hoshino, T. Mitsui, and H. Tanaka, *J. Phys. Soc. Jpn.* **61**, 275 (1992).
- ⁴¹ J. B. Forsyth, R. M. Ibberson, Yu. M. Tsipenyuk, and S. V. Petrov, *Phase Transit.* (to be published).
- ⁴² I. E. Dzyaloshinsky, *Zh. Eksp. Teor. Fiz.* **47**, 992 (1964)
- [*Sov. Phys. JETP* **20**, 665 (1965)]; P. Bak and J. v. Boehm, *Phys. Rev. B* **21**, 5297 (1980).
- ⁴³ V. L. Pokrovsky and A. L. Talapov, *Zh. Eksp. Teor. Fiz.* **75**, 1151 (1978) [*Sov. Phys. JETP* **48**, 579 (1978)].
- ⁴⁴ A. E. Jacobs, T. Nikuni, and H. Shiba, *J. Phys. Soc. Jpn.* **62**, 4066 (1993).